

Interaction of Substance P with Phospholipid Bilayers: A Neutron Diffraction Study

Jeremy P. Bradshaw,^{*,#} Sarah M. A. Davies,^{*} and Thomas Hauss[§]

^{*}Department of Preclinical Veterinary Sciences, Royal (Dick) School of Veterinary Sciences, University of Edinburgh, Summerhall, Edinburgh EH9 1QH, Scotland, United Kingdom, [#]Department of Biochemistry, University of Edinburgh School of Medicine, Edinburgh EH8 9XD, Scotland, United Kingdom, and [§]Hahn Meitner Institut, D-14 109 Berlin, Germany

ABSTRACT Neutron diffraction has been used to study the membrane-bound structure of substance P (SP), a member of the tachykinin family of neuropeptides. The depth of penetration of its C-terminus in zwitterionic and anionic phospholipid bilayers was probed by specific deuteration of leucine 10, the penultimate amino acid residue. The results show that the interaction of SP with bilayers, composed of either dioleoylphosphatidylcholine (DOPC), or a 50:50 mixture of DOPC and the anionic phospholipid dioleoylphosphatidylglycerol (DOPG), takes place at two locations. One requires insertion of the peptide into the hydrophobic region of the bilayer, the other is much more peripheral. The penetration of the peptide into the hydrophobic region of the bilayer is reflected in a marked difference in the water distribution profiles. SP is seen to insert into DOPC bilayers, but a larger proportion of the peptide is found at the surface when compared to the anionic bilayers. The positions of the two label populations show only minor differences between the two types of bilayer.

INTRODUCTION

Substance P (SP) belongs to the tachykinin family, a group of six small amphipathic peptides that bind to G-protein coupled receptors. The receptors are found in a wide range of tissues including the central and peripheral nervous systems and the gastrointestinal tract. The tachykinin family of peptides shares a common C-terminus, FxGLM-NH₂, where *x* is F or V in mammals.

The ligand-binding sites of tachykinin receptors appear to involve both the extracellular loops and the transmembrane domains (Yokota et al., 1992). An address-message model (Schwyzer, 1987) has been proposed where the flexible cationic N-terminal region of SP, or “address domain,” is responsible for receptor selectivity, while the structurally extended and conserved hydrophobic C-terminal delivers the message. The proposed mechanism involves an interaction between tachykinin and phospholipids which results in insertion of the C-terminal amino acids into the lipid bilayer, followed by lateral diffusion of the peptide to reach the ligand-binding site of a membrane-bound receptor. Seelig et al. (1996) have presented an argument against the proposed membrane-mediated receptor mechanism, based on their observation that an SP analog with a charged C-terminus, which they suggest would not insert into the hydrophobic core of membranes, still shows SP agonist activity. However, the central role of peptide-lipid interactions in the proposed scheme is supported by a number of

observations that show the conformation of SP is determined by the nature of its local chemical environment (e.g., Chuen-Shang et al., 1982; Chassaing et al., 1986; Woolley and Deber, 1987; Convert et al., 1991).

There have been several biophysical studies comparing the structure of SP in zwitterionic and anionic lipid environments. Based on monolayer expansion measurements, Seelig and MacDonald (1989) concluded that SP does insert into monolayers containing negatively charged 1-palmitoyl-2-oleoyl-phosphatidylglycerol (POPG), but does not insert into zwitterionic monolayers composed of 1-palmitoyl-2-oleoyl-phosphatidylcholine (POPC).

Wu and Yang (1981) have proposed that polypeptides with a helix-forming potential can only assume a helical conformation in hydrophobic environments, such as the core of biological membranes, where the milieu enhances the intramolecular hydrogen bonding necessary for the stabilization of these structures. This argument has been developed (Wu et al., 1982) with the demonstration that such helical structures can only form by interaction with lipids when the peptide carries either no charge or charges opposite to those of the polar headgroup of the lipid. When this principle was applied to SP circular dichroism (CD) spectra revealed an unordered structure in water or phosphatidylcholine, but a partial helix in negatively charged phosphatidylserine or sodium dodecylsulfate (SDS).

In contrast, Woolley and Deber (1987) have reported CD data from SP in the presence of SDS, lysophosphatidylcholine, and lysophosphatidylglycerol micelles that show that the induced helical structure is independent of the lipid headgroup type. Keire and Fletcher (1996) also concluded from CD and ¹H-NMR studies that the conformation of SP is independent of lipid headgroup type. They calculated SP structures to 1–2 Å resolution from NMR measurements of SP in three different solution environments (SP/dodecylphosphocholine, SP/dodecylphosphocholine/NaCl, and

Received for publication 20 January 1998 and in final form 20 May 1998.

Address reprint requests to Dr. Jeremy P. Bradshaw, Dept. of Preclinical Veterinary Sciences, Royal (Dick) School of Veterinary Sciences, University of Edinburgh, Summerhall, Edinburgh EH9 1QH, Scotland, United Kingdom. Tel.: 0131-650-6139; Fax: 0131-650-6576; E-mail: j.bradshaw@ed.ac.uk.

© 1998 by the Biophysical Society

0006-3495/98/08/889/07 \$2.00

SP/SDS/NaCl) and found them all to be similar. The structure they determined for SP is shown in Fig. 1.

Against this background, the aim of the study described here was to test the hypothesis that SP interacts with biological phospholipids in such a way that the "message" portion of the peptide is delivered at a specific depth, or "address," within a bilayer. In order that the findings might also contribute to the debate on whether the membrane interaction of SP is phospholipid-dependent, two different bilayer compositions were used. In one system the bilayers were composed of the zwitterionic phospholipid dioleoylphosphatidylcholine (DOPC); the other system contained a 50:50 (mol) mixture of DOPC and the anionic phospholipid dioleoylphosphatidylglycerol (DOPG).

MATERIALS AND METHODS

Sample preparation

DOPC and DOPG were purchased from Avanti Polar Lipids (Alabaster, AL) and used without further purification. The 11 amino acid peptide (RPKPQQFFGLM-NH₂) was synthesized by Albachem Ltd. (26 Craigleith View, Edinburgh, EH4 3JZ, Scotland, UK). The synthesis was carried out on an Applied Biosystems 430A instrument, using Fmoc chemistry with the side chain protecting groups selected as tBu (Ser, Thr) and OtBu (Glu). The completed peptide was cleaved with a solution of TFA/H₂O (95:5) plus scavengers (ethanedithiol/thioanisole/triisopropanesilane) and the solution was evaporated under vacuum. The peptide was purified by reverse phase HPLC and characterized by mass spectra (MALDI, PerSeptive Biosystem laserTec), amino acid analysis (LKB 4150 α amino acid analyzer) and analytical HPLC. Two batches of peptide were produced, one undeuterated and one containing deuterated leucine (10 deuterons) at position 10. The purity of each peptide was above 95%, as determined by analytical HPLC, mass spectrometry, and amino acid analysis. Twenty-milligram samples of lipid, some of which contained 3% (mol) peptide, were deposited on quartz microscope slides (75 mm \times 25 mm) using an

artist's airbrush. The spraying solvent was methanol. The slides were placed in a vacuum desiccator for 12 h to remove all traces of the solvent before rehydration for 24 h at 25°C in an atmosphere of 100% relative humidity.

Neutron data collection

Neutron diffraction measurements were carried out on the V1 membrane diffractometer at the Berlin Neutron Scattering Centre, Germany. The sample environment was a standard aluminum can, in which temperature control is achieved by circulating water through an integral water jacket, and humidity control by changing the solution in two Teflon water baths at the base of the can. These water baths contained pure water, at one of three isotopic compositions: 0%, 50%, or 100% ²H₂O. Using the ²H₂O/H₂O exchange technique, every sample was measured at all three ²H₂O concentrations. At each change of solvent, the sample was first dried out under vacuum, then rehydrated in an atmosphere saturated with water at the new isotopic composition for at least 24 h. All samples were run at 25°C. The scanning protocol consisted of sequential θ scans around the predicted Bragg angle for each order. Each scan covered the angular range ($\theta_n - 0.5^\circ$) to ($\theta_n + 0.5^\circ$), where θ_n is the Bragg angle for the n th order of lamellar diffraction.

Neutron data analysis

The 2-dimensional array of detector counts for each frame of neutron diffraction data was corrected for variations in pixel response by division by a corresponding array of data recorded from water. The complete set of frames from each scan was then collapsed into a linear spectrum and combined to generate a pseudo θ - 2θ scan. Up to this stage of the analysis, all calculations were carried out using the V1 instrument software.

The background around each peak was fitted and subtracted using SigmaPlot v3.0 (Jandel Scientific Software GmbH), a commercial spreadsheet and graphs package. Gaussian curves were then fitted to the Bragg reflections and the angular position, width, and area of each peak were recorded. Absorption and Lorentz corrections were applied and the intensities square-rooted to produce structure factor amplitudes. The relative scaling of the different data sets and the phases of each of their orders were determined by least-squares fitting to straight line functions, as shown in Fig. 2.

The D -repeat of each sample was calculated by least-squares fitting of the observed values of 2θ to the Bragg equation, $n\lambda = 2D \cdot \sin(\theta_{n+s})$, where s is the angular offset (misalignment) of the detector.

The data were placed on a "relative absolute" scale (Wiener et al., 1991; Wiener and White, 1991; Jacobs and White, 1989) using the known neutron scattering densities of ²H and H to scale the [DOPC + ²H₂O] - [DOPC + H₂O] differences and the [DOPC + (²H₁₀-Leu)-SP] - [DOPC + SP] differences. This method requires knowledge of the molar percentage of water in the samples, which was determined as described below.

Gaussian distributions were fitted to the deuterated leucine sites by least-squares methods. The process was carried out in reciprocal space, whereby each Gaussian model is tested by comparing its calculated structure factors to the differences between observed structure factors for deuterated and undeuterated peptides.

Determination of water content

The neutron diffraction sample preparation was repeated using ¹⁴C-labeled DOPC and tritiated water so that scintillation counting could be used to determine the water/lipid molar ratio. Microscope coverslips (22 \times 22 mm) were cut in half to provide a suitable substrate which would fit into a standard scintillation counter tube. To give the same sample thickness, ~5.0 mg lipid was spread on each half-coverslip. After vacuum dehydration and rehydration for 24 h, in small batches, at 25°C, the coverslips were quickly transferred to tubes of scintillant. ¹⁴C and ³H activity were measured using a Packard 1900CA Liquid Scintillation Counter. Control sam-

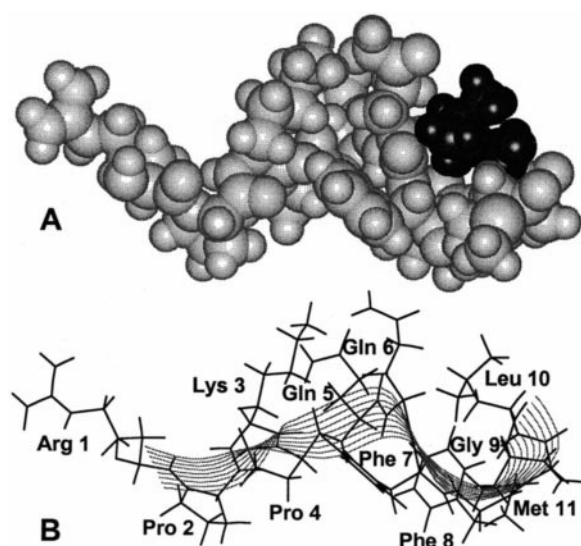


FIGURE 1 The structure of substance P as determined by Keire and Fletcher (1996), as used in the analysis of neutron diffraction data as described here. Both space-filling (A) and wire-model (B) representations are shown. Leucine 10, the residue that was deuterated in some of the peptide used in this study, is indicated in black.

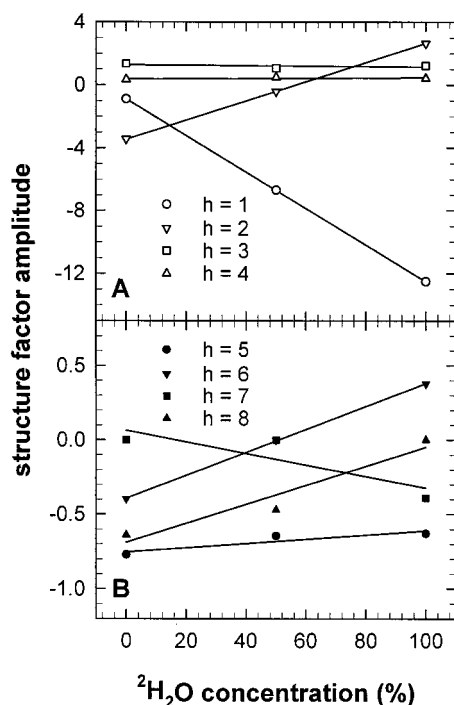


FIGURE 2 An example of the structure factors and their phase assignment using $\text{H}_2\text{O}/^2\text{H}_2\text{O}$ exchange, in this instance DOPC with 50% (mol) DOPG and 3.0% (mol) substance P. Each order has been fitted (least squares) to a straight line with negative slope for odd-numbered orders and positive slope for even-numbered orders. This relationship breaks down at higher-order numbers, indicating that, at higher resolution, the shape of the water distribution can no longer be described as a single Gaussian distribution. For clarity, the eight orders are split between two plots: (A), first four orders; (B), orders five to eight on an enlarged vertical scale. The phasing of orders seven and eight is uncertain. All subsequent calculations only used the first six orders.

ples containing tritiated water (1.2 μl) or ^{14}C -DOPC, equivalent to 5.0 mg experimental phospholipid, were used to calibrate the scintillation counter channel and cross-channel response. Clean coverslips served as controls for the experiment, to ensure that the amount of water condensing on the reverse side was negligible.

RESULTS

Table 1 shows the neutron structure factors of DOPC bilayers with 3% (mol) SP or $(^2\text{H}_{10}\text{-Leu})\text{-SP}$ and bilayers of DOPC with 50% (mol) DOPG and 3% (mol) SP or $(^2\text{H}_{10}\text{-Leu})\text{-SP}$. Fig. 2 shows an example of the structure factor data, scaled and phased so that straight lines pass through each order of the structure factors from each $^2\text{H}_2\text{O}/\text{H}_2\text{O}$ exchange series. Neutron scattering density profiles, calculated by Fourier transformation structure factors, are shown in Figs. 3 to 5.

The D -repeats of the various samples were 53.2 ± 0.4 Å, 55.4 ± 1.0 Å, and 54.8 ± 1.0 Å for the pure DOPC, DOPC with 3% (mol) SP, and 3% (mol) $(^2\text{H}_{10}\text{-Leu})\text{-SP}$, and 52.6 ± 0.9 Å, 55.0 ± 1.0 Å, and 55.4 ± 1.0 Å for the corresponding DOPC/DOPG samples. These differences in D -repeat, though well within the generally accepted range

(up to 1 Å), are a potential source of error when the structure factors, or profiles calculated from them, are subtracted from each other. This error is most marked in the 100% $^2\text{H}_2\text{O}$ structure factors, where even a small difference in the amount of water present can represent a considerable change in the scattering density of that region of the sample. The level of deuteration of the peptide in this study is relatively low when compared to the $^2\text{H}_2\text{O}\text{-H}_2\text{O}$ differences so, in order to reduce the effect of these errors, all profiles and subtractions were calculated at 8.07% $^2\text{H}_2\text{O}$, at which isotopic composition water has a net scattering density of zero.

The mosaic spread of all samples used in the analysis was less than 0.5° (full width at half height). There was no significant variation between the different samples. The water content of the samples, measured by scintillation counting, was DOPC, 26.08 waters per lipid; DOPC + DOPG, 30.49; DOPC + SP, 26.35; DOPC + DOPG + SP, 28.40. The maximum error in these measurements was estimated to be ± 1.0 waters per lipid.

Two different model-fitting approaches were taken in order to interpret the neutron data. The simpler of the two types of model was two Gaussian distributions (and their mirror images in the centrosymmetric unit cell). The Gaussian distributions were fitted to the observed differences between deuterated and undeuterated SP, the variables being height, width, and position along the bilayer normal. The fitting process was carried out in reciprocal (diffraction) space by comparing the calculated structure factors of each model to the observed difference structure factors. The results of this approach are summarized in Table 2.

The second approach was used to determine the location of the whole peptide relative to the bilayer. It was essentially an elaboration of the Gaussian technique in which the neutron scattering profile of SP was calculated by combining the molecular coordinates of the peptide from a recent NMR structure determination (Keire and Fletcher, 1996) with the coherent scattering length of its component atoms. A Gaussian distribution, the integral of which was equal to the scattering length of that atom, represented each atom. In the case of the deuterium label distributions, the scattering length of all atoms other than the deuteriums was set to zero. The scattering length of the deuteriums was set at 1.041×10^{-12} cm, equivalent to the difference between the scattering lengths of ^1H and ^2H . The best fit to the label distribution in DOPC bilayers was found to be when the center of the whole peptide was 12.0 Å and 24.4 Å from the center of the bilayer. The axis of the peptide was parallel to the bilayer normal for the inserted peptide and perpendicular to the normal for the surface peptide. In this calculation a smearing factor of 5.3 Å was applied to each atom of the inserted peptide and 4.4 Å for the surface peptide. The corresponding figures for the DOPC/DOPG bilayers were 14.2 Å and 24.5 Å from the center of the bilayer, with a 4.0 Å smearing factor for both populations of peptide. The results of both model-fitting approaches are summarized in Figs. 4 and 5. It should be noted that the figures show a

TABLE 1 Experimentally determined, corrected, and scaled neutron structure factors of stacked bilayers of DOPC, DOPC with 3% (mol) SP or ($^2\text{H}_{10}$ -Leu)-SP, DOPC with 50% (mol) DOPG and DOPC with 50% (mol) DOPG, and 3% (mol) SP or ($^2\text{H}_{10}$ -Leu)-SP.

Sample	F(1)	F(2)	F(3)	F(4)	F(5)	F(6)	F(7)	F(8)
DOPC, 3% (mol) Substance P, 0% $^2\text{H}_2\text{O}$								
(1)	-0.68 ± 0.05	-3.64 ± 0.11	1.46 ± 0.11	2.09 ± 0.11	-0.86 ± 0.05	-0.65 ± 0.05	± 0.69 ± 0.05	± 0.64 ± 0.05
DOPC, 3% (mol) Substance P, 100% $^2\text{H}_2\text{O}$								
(2)	-13.27 ± 0.25	3.02 ± 0.10	0.75 ± 0.05	0.20 ± 0.05	1.03 ± 0.08	0.58 ± 0.05	± 0.57 ± 0.05	± 0.78 ± 0.05
DOPC, 3% (mol) ($^2\text{H}_{10}$ -Leu-10)-Substance P, 0% $^2\text{H}_2\text{O}$								
(3)	-0.52 ± 0.11	-2.85 ± 0.11	0.98 ± 0.11	0.80 ± 0.11	-0.72 ± 0.11	-0.85 ± 0.11	± 0.93 ± 0.11	± 0.82 ± 0.11
DOPC, 3% (mol) ($^2\text{H}_{10}$ -Leu-10)-Substance P, 100% $^2\text{H}_2\text{O}$								
(4)	-13.14 ± 0.25	3.55 ± 0.10	0.75 ± 0.05	-0.30 ± 0.05	1.22 ± 0.08	0.38 ± 0.05	± 0.55 ± 0.05	± 0.75 ± 0.05
DOPC+DOPG (50:50), 3% (mol) Substance P, 0% $^2\text{H}_2\text{O}$								
(5)	-0.90 ± 0.05	-3.45 ± 0.10	1.28 ± 0.08	0.38 ± 0.05	-0.71 ± 0.05	0.39 ± 0.05	± 0.06 ± 0.05	± 0.69 ± 0.05
DOPC+DOPG (50:50), 3% (mol) Substance P, 100% $^2\text{H}_2\text{O}$								
(6)	-12.51 ± 0.25	2.64 ± 0.10	1.15 ± 0.08	0.45 ± 0.05	-0.47 ± 0.05	-0.38 ± 0.05	± 0.32 ± 0.05	± 0.05 ± 0.05
DOPC+DOPG (50:50), 3% (mol) ($^2\text{H}_{10}$ -Leu-10)-Substance P, 0% $^2\text{H}_2\text{O}$								
(7)	-0.43 ± 0.05	-4.19 ± 0.15	-0.68 ± 0.05	-0.93 ± 0.05	0.00	0.68 ± 0.05	± 0.90 ± 0.05	± 0.79 ± 0.05
DOPC+DOPG (50:50), 3% (mol) ($^2\text{H}_{10}$ -Leu-10)-Substance P, 100% $^2\text{H}_2\text{O}$								
(8)	-12.05 ± 0.25	3.03 ± 0.10	-0.81 ± 0.05	-0.56 ± 0.05	0.00	-0.14 ± 0.05	± 0.01 ± 0.05	± 0.16 ± 0.05
DOPC, 0% $^2\text{H}_2\text{O}$								
(9)	-8.14 ± 0.20	-19.37 ± 0.26	10.20 ± 0.20	-3.63 ± 0.15	-3.33 ± 0.15	0.00	0.00	± 0.75 ± 0.05
DOPC, 100% $^2\text{H}_2\text{O}$								
(10)	-161.48 ± 1.00	28.29 ± 0.30	5.58 ± 0.15	8.51 ± 0.20	-8.53 ± 0.20	0.00	± 5.30 ± 0.15	± 1.69 ± 0.08
DOPC+DOPG (50:50), 0% $^2\text{H}_2\text{O}$								
(11)	-14.67 ± 0.25	-30.93 ± 0.30	17.80 ± 0.26	-2.45 ± 0.10	2.95 ± 0.10	-6.19 ± 0.18	± 4.57 ± 0.15	± 4.15 ± 0.15
DOPC+DOPG (50:50), 100% $^2\text{H}_2\text{O}$								
(12)	-166.76 ± 1.00	41.02 ± 0.35	-12.91 ± 0.25	5.99 ± 0.15	4.06 ± 0.15	-5.30 ± 0.15	± 4.31 ± 0.15	± 0.83 ± 0.06

The measurements were made at 25°C and 100% relative humidity. The phasing of orders seven and eight is uncertain. All subsequent calculations used only the first six orders. The errors are related to the deviations of the observed points to straight lines fitted through structure factors at three $^2\text{H}_2\text{O}$ concentrations, as in Fig. 2.

comparison of the calculated and observed scattering profiles in real space; the actual model fitting was carried out in reciprocal space. Also shown is the calculated scattering profile of SP, using the peptide locations and smearing factors determined by the deuterium peak model fitting.

DISCUSSION

DOPC with DOPG bilayers

Figs. 4 and 5 and Table 2 clearly show that the interaction of SP with the phospholipid membranes employed in this study takes place at two locations. One involves insertion of the peptide into the hydrophobic region of the bilayer, the other is much more peripheral. The penetration of the peptide into the hydrophobic region of the bilayer is reflected in a marked difference in the water distribution profiles (Fig. 3) in the presence of peptide. These profiles which, more correctly, represent not just the water, but also deuterium-

exchanged sites on the peptide, each show a large presence of deuterium right across the bilayer profile.

The difference profiles, showing the bilayer distribution of deuterated leucine on SP, clearly demonstrate two populations of peptide. To interpret these findings in more detail, a model-fitting approach was employed, based on a recently published NMR structure of micelle-bound SP (Keire and Fletcher, 1996), in which the peptide/lipid ratio was similar to that used in the neutron work. The NMR structure was positioned on the bilayer normal, its exact location being determined by fitting the calculated neutron scattering from the deuterium label sites to the observed scattering in difference profiles. This approach is particularly appropriate for the deeper location, as it positions the peptide relative to the surrounding phospholipids in a very similar manner to that described in the NMR work. The conformation of SP in the peripheral location is much less certain, but for want of a better alternative, we have again

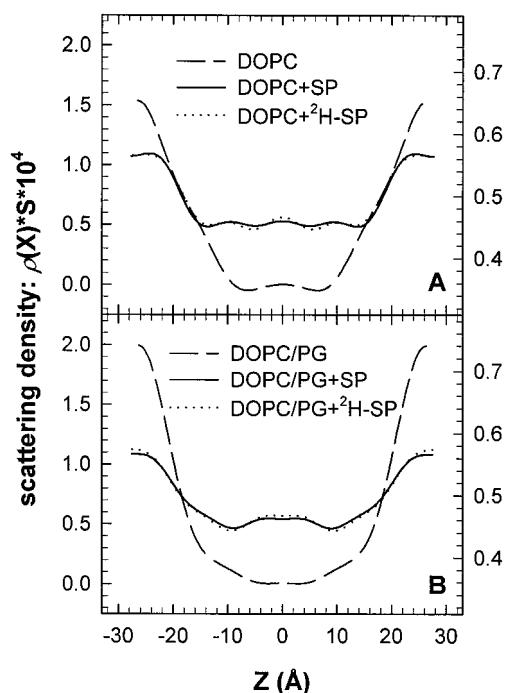


FIGURE 3 The distribution of deuterium, introduced in the form of 50% $^2\text{H}_2\text{O}$, within and between bilayers of (A) DOPC (dashed line, left hand scale), DOPC with 3.0% (mol) substance P (solid line, right hand scale), and DOPC with 3.0% (mol) $(^2\text{H}_{10}\text{-Leu-10})$ -substance P (dotted line, right hand scale); (B) DOPC with 50% (mol) DOPG (dashed line, left hand scale), DOPC with 50% (mol) DOPG and 3.0% (mol) substance P (solid line, right hand scale), and DOPC with 50% (mol) DOPG and 3.0% (mol) $(^2\text{H}_{10}\text{-Leu-10})$ -substance P (dotted line, right hand scale).

used the Keire structure in our interpretation, but oriented with its long axis parallel to the bilayer. In support of this, it should be noted that the work by Keire and Fletcher only presents one structure for the peptide, while it is quite feasible that their samples also contained two populations of peptide.

An alternative explanation for the two deuterium peaks would be to suggest that the peptide aggregates in an anti-parallel manner. Three arguments refute this suggestion. Firstly, the relative sizes of the two populations of label are not stoichiometric and differ between the two types of bilayer studied. Secondly, in order to insert in the alternative (antiparallel) direction, the peptide would need to introduce its N-terminus, together with its three positive charges, into the hydrophobic core of the bilayer. Finally, the Fourier-transform infrared study of Choo and co-workers (1994) reported that SP aggregates in the presence of charged lipids, but not in an anti-parallel manner.

Once the peptide structures had been located and oriented using the deuterium label information, it was a straightforward matter to calculate the contribution of scattering from all peptide atoms to the neutron scattering profiles. Fig. 5 B illustrates the comparison of such a profile to the corresponding profile derived from observed data, using the difference method. Reference to the figures shows that the calculated scattering profile is relatively low and feature-

less. Thus any of a number of surface peptide conformations could have been used in the calculation without seriously affecting the results. A comparison of the profiles shows that the majority of the scattering difference comes from neither the peptide nor the water, since the profile corresponds to a bilayer with 8.07% $^2\text{H}_2\text{O}$, at which isotopic composition water has a net coherent neutron scattering density of zero. The differences between the profiles can only, therefore, represent rearrangements of the phospholipid. Wu and co-workers (1995) have reported membrane thinning as a direct result of peptide incorporation into phospholipid bilayers. It is quite possible that the insertion of SP may have a similar effect on phospholipids.

DOPC bilayers

To contribute to the discussion on whether SP inserts into zwitterionic membranes, neutron measurements were also performed on DOPC bilayers, some of which contained SP at 3.0% (mol). The results, summarized in Table 2, show that SP does indeed insert into DOPC bilayers, but it is interesting that more of the peptide is found at the surface when compared to the anionic bilayers.

In comparison to the DOPC results, the positions of the two label populations show only minor differences. Indeed, it is noticeable in Fig. 3 that the water distribution between adjacent bilayers is wider in those bilayers containing only DOPC (A), indicating that the anionic bilayers are wider than the zwitterionic ones. For practical reasons, the location of the label sites in Table 2 is expressed in terms of distance from the center of the bilayer. Were it possible to present the results as distance from the bilayer surface, it is likely that the difference between the two lipids would be even smaller.

Keire and Fletcher (1996) have reported that the conformation of SP, as determined by $^1\text{H-NMR}$, does not differ significantly between anionic and zwitterionic micelles. In both systems they observed a similar conformation for association of the QQFFGLM residues with lipid micelles. The only variations in structure were observed in the N-terminal residues, RPKP. This was interpreted as indicating that the structure of SP at a micelle surface is determined largely by hydrophobic forces, while the electrostatic interactions determine the amount of SP that is bound. This interpretation is in close agreement with the neutron results reported here.

However, the neutron data do not appear to agree with the monolayer expansion measurements of Seelig and MacDonald (1988), who concluded that SP does not insert into zwitterionic monolayers. It should be noted, however, that both the lipids used (DOPC instead of POPC) and their arrangement (bilayers instead of monolayers) differs between the two studies. It is arguable that monolayers do not present an accurate representation of bilayers, especially when considering the insertion of molecules into the bilayer center, or beyond. Conversely, it is possible that the nature

TABLE 2 Gaussian models of deuterium label distribution of 3.0% (mol) ($^2\text{H}_{10}$ -Leu-10)-Substance P in bilayers of DOPC or DOPC+DOPG (50:50)

Site	Parameter	DOPC	Distribution	DOPC+DOPG	Distribution
1	Position*	$6.61 \pm 0.22 \text{ \AA}$	$57.5 \pm 5.5\%$	$8.82 \pm 0.22 \text{ \AA}$	$65.6 \pm 5.5\%$
	Width [#]	$9.18 \pm 0.88 \text{ \AA}$		$6.99 \pm 0.33 \text{ \AA}$	
2	Position*	$22.04 \pm 0.22 \text{ \AA}$	$42.5 \pm 5.5\%$	$22.34 \pm 0.83 \text{ \AA}$	$34.3 \pm 5.5\%$
	Width [#]	$8.27 \pm 0.83 \text{ \AA}$		$7.54 \pm 0.66 \text{ \AA}$	

The position, width, and size of Gaussian distributions were fitted, in reciprocal space, to difference neutron structure factors. Six orders of diffraction were used in the fitting procedure.

* The position of each label site is expressed as distance from the center of the bilayer.

[#] The width is the full width at half height.

of the neutron samples, in which adjacent bilayers are separated by a narrow (15–20 Å) water channel, artificially increases the concentration of peptide close to the surface of the bilayers. This contrasts with the monolayer expansion system, in which the peptide was introduced into the aqueous layer. The binding of SP to the monolayer surface was reported to be dominated by electrostatic interaction. Therefore, an anionic surface would be predicted to attract the positively charged peptide much more readily than would a zwitterionic surface.

The message-address model of Schwyzer (1987) requires that each tachykinin interacts in a tightly controlled manner with phospholipid membranes. For the message to be de-

livered at the correct address, the C-terminal portion of the peptide must be located at a specific depth within the bilayer, irrespective of its phospholipid composition. While the neutron measurements reported here can neither support nor refute such a model, they clearly demonstrate that SP is

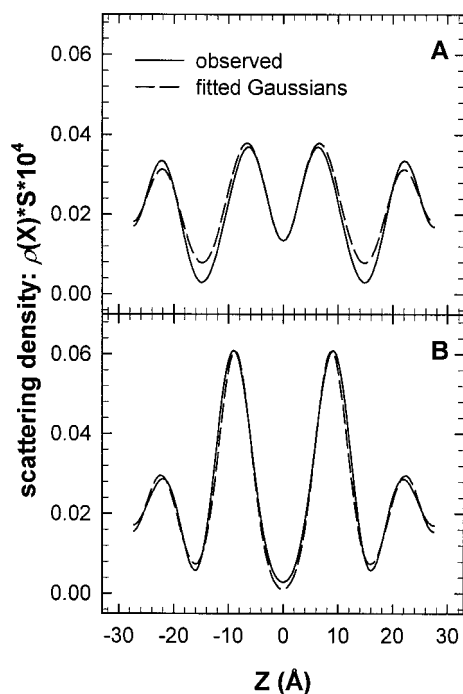


FIGURE 4 Model-fitting (1). Difference neutron scattering density profiles, calculated from six orders of diffraction, showing the distribution of deuterium in 3% (mol) ($^2\text{H}_{10}$ -Leu-10)-substance P in (A) DOPC bilayers and (B) DOPC/DOPG bilayers (50:50). The subtraction was carried out using structure factors representing 8.07% $^2\text{H}_2\text{O}$, to reduce the effect of slight differences in hydration level between the samples. Each panel also shows (dashed line) the sum of two pairs of Gaussian distributions, fitted to the difference data in reciprocal space (six orders of diffraction).

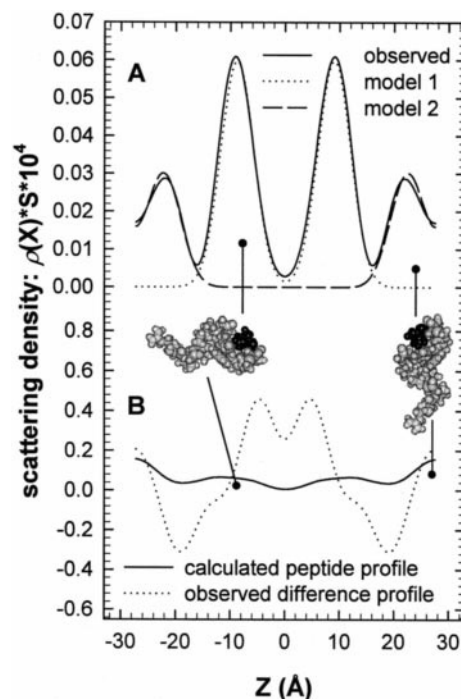


FIGURE 5 Model-fitting (2). (A) The distribution of deuterium in 3% (mol) ($^2\text{H}_{10}$ -Leu-10)-substance P in DOPC/DOPG bilayers (50:50), shown as difference neutron scattering density profiles calculated from six orders of diffraction. Also shown are the calculated neutron scattering density distributions for deuterium in 3% (mol) ($^2\text{H}_{10}$ -Leu-10)-substance P, using the NMR structure for SP of Keire and Fletcher (1996). In Model 1 the peptide is arranged perpendicular to the bilayer and in Model 2 parallel to the bilayer, as indicated. (B) Predicted neutron scattering profile of 3% (mol) substance P (solid line) calculated using the whole Keire and Fletcher structure, with the peptide arranged in two populations arranged as in (A). The dotted line is the observed neutron scattering density profile at 8.07% $^2\text{H}_2\text{O}$, calculated by subtracting the DOPC/DOPG profile from the (SP + DOPC/DOPG) profile. The two profiles shown are very different, indicating that the dotted line includes scattering contributions from sources other than the peptide alone. Since the dotted profile represents a bilayer at 8.07% $^2\text{H}_2\text{O}$, at which isotopic composition water is effectively invisible to neutrons, the difference between the predicted and observed profiles can only be caused by rearrangements of the phospholipids.

able to interact with both zwitterionic and anionic membranes in such a way that the C-terminus of the peptide is positioned at a tightly controlled depth below the membrane surface. Moreover, in agreement with other studies, the proportion of peptide that penetrates the membrane is shown to be dependent upon the phospholipid composition of the bilayer.

The experiments at BENSCH in Berlin were supported by the European Commission through the TMR (Training and Mobility of Researchers) Programme, "Access to large-scale facilities" (Contract: ERB CHGE CT 920014). S.M.A.D. holds a Wellcome Trust Veterinary Research Scholarship.

REFERENCES

- Chassaing, G., O. Convert, and S. Lavielle. 1986. Preferential conformation of substance P in solution. *Eur. J. Biochem.* 154:77–85.
- Choo, L.-P., M. Jackson, and H. H. Mantsch. 1994. Conformation and self-association of the peptide hormone substance P: Fourier-transform infrared spectroscopic study. *Biochem. J.* 301:667–670.
- Chuen-Shang, C. W., A. Hachimori, and J. T. Yang. 1982. Lipid-induced ordered conformation of some peptide hormones and bioactive oligopeptides: predominance of helix over β form. *Biochemistry*. 21: 4556–4562.
- Convert, O., H. Duplaa, S. Lavielle, and G. Chassaing. 1991. Influence of the replacement of amino-acid by its d-enantiomer in the sequence of substance-P. 2. Conformational-analysis by NMR and energy calculations. *Neuropeptides*. 19:259–270.
- Jacobs, R. E., and S. H. White. 1989. The nature of the hydrophobic binding of small peptides at the bilayer interface: implications for the insertion of transbilayer helices. *Biochemistry*. 28:3421–3437.
- Keire, D. A., and T. G. Fletcher. 1996. The conformation of substance P in lipid environments. *Biophys. J.* 70:1716–1727.
- Schwyzler, R. 1987. Membrane-assisted molecular mechanism of neurokinin receptor subtype selection. *EMBO J.* 6:2255–2259.
- Seelig, A., T. Alt, S. Lotz, and G. Holzemann. 1996. Binding of substance P agonists to lipid membranes and to the neurokinin-1 receptor. *Biochemistry*. 35:4365–4374.
- Seelig, A., and P. M. MacDonald. 1989. Binding of a neuropeptide, substance P, to neutral and negatively charged lipids. *Biochemistry*. 28:2490–2496.
- Wiener, M. C., G. I. King, and S. H. White. 1991. Structure of fluid DOPC bilayer determined by joint refinement of x-ray and neutron data. *Biophys. J.* 62:2762–2772.
- Wiener, M. C., and S. H. White. 1991. Fluid bilayer structure determination by the combined use of x-ray and neutron diffraction. *Biophys. J.* 59:162–185.
- Woolley, G. A., and C. M. Deber. 1987. Peptides in membranes—lipid-induced secondary structure of substance-P. *Biopolymers*. 26: S109–S121.
- Wu, C. C., A. Hachimori, and J. T. Yang. 1982. Lipid-induced ordered conformation of some peptide hormones and bioactive oligopeptides: predominance of helix over β form. *Biochemistry*. 21:4556–4562.
- Wu, Y. L., K. He, S. J. Ludtke, and H. W. Huang. 1995. X-ray-diffraction study of lipid bilayer-membranes interacting with amphiphilic helical peptides—diphytanoyl phosphatidylcholine with alamethicin at low concentrations. *Biophys. J.* 68:2361–2369.
- Wu, C. C., and J. T. Yang. 1981. Sequence-dependent conformations of short polypeptides in a hydrophobic environment. *Mol. Cell. Biochem.* 40:109–122.
- Yokota, Y., C. Akazawa, H. Ohkubo, and S. Nakanishi. 1992. Delineation of structural domains involved in the subtype specificity of tachykinin receptors through chimeric formation of substance-P substance-K receptors. *EMBO J.* 11:3585–3591.